Celal Bayar University Journal of Science

The Effect of Sintering Graphene and SiC Reinforced Aluminum Hybrid Composites with Ultra-High Frequency Induction Heating System (UHFIS) on Mechanical Properties

Büşranur Keser[1], Gürkan Soy[2], Selda Kayral[3]*

[1,3]Manisa Celal Bayar University, Department of Mechanical Engineering, 45400 Manisa, Türkiye.
[2]Manisa Celal Bayar University, Department of Machine and Metal Technologies, 45400 Manisa, Türkiye.
* selda.akgun@cbu.edu.tr
* Orcid No: 0000-0003-1971-1550

Received: March 27, 2025
Accepted: June 29, 2025
DOI: 10.18466/cbayarfbe.1666717

Abstract

Hybrid composites have two or more reinforcement ratios, and they are among the preferred materials in many engineering applications due to their unique properties, such as lightness, low cost, easy applicability, and high strength. This study investigated the effect of sintering aluminum matrix graphene (0.1% and 0.5%) and SiC (10% and 20%) reinforced hybrid composite with an ultra-high frequency induction heating system on mechanical and physical properties. Powder mixtures were prepared using a three-dimensional mixing system were prepared according to the experimental design created by the Taguchi method at three different temperatures (580, 600, and 620 ℃), three different pressures (80, 90, and 100 bar), and three different sintering times (5, 7 and 10 min). It was produced, and its hardness, density, and microstructure were examined. ANOVA analysis was performed on the results obtained and a mathematical model was created. As a result of the experiments, the highest hardness value of the 0.1% graphene and 10% SiC reinforced hybrid composite was 90.4 HB at 100 bar pressure, 10 min sintering time and 580 ℃ sintering temperature, and the highest hardness value of the 0.5% graphene and 20% SiC reinforced composite was 100 bar. The pressure was obtained as 103.5 HB at 5 min sintering time and 600 ℃ sintering temperature.

Keywords: Aluminum, Graphene, Hybrid Composites, SiC, Taguchi, Ultra High Frequency Induction Heating System.

1. Introduction

Today's competitive environment requires better quality products to be offered at lower costs. Since the need for low-density (lightweight), robust, and high-strength materials is increasing daily in many technical applications in the industry, studies for developing new-generation materials are gaining momentum as a subject of interest for researchers working in materials **[1]**. In this sense, metal matrix composites (MMCs) have been developed to meet many mechanical and physical properties that a single material cannot provide **[2]**.

Pure Aluminum is the most widely used matrix material among MMCs. Aluminum alloys are used in advanced applications due to their low density, ability to increase strength through precipitation hardening, high corrosion resistance, high thermal and electrical conductivity, easy processability and ease of supply, which makes Aluminum superior to competing materials **[1, 2]**. These superior physical and mechanical properties make them attractive materials for automotive electronics, machine manufacturing and aerospace applications **[3]**. The mechanical and physical properties of pure Aluminum are given in Table 1.

Table 1. Properties of Pure Aluminum **[4]**.

Material	Pure Aluminum
Density (g/cm^3)	2.7
Modulus of Elasticity (GPa)	68.3
Hardness (HB)	21
Tensile Strength (MPa)	90
Melting Temperature (°C)	660.2
Poisson's ratio	0.34
Crystal Structure	YMK

Celal Bayar University Journal of Science
Volume 21, Issue 4, 2025, p 118-127
Doi: 10.18466/cbayarfbe.1666717

Since conventional metals and alloys are inadequate under extreme conditions requiring high stiffness and strength, MCC's contain reinforcement groups, different ceramic-based reinforcements such as B_4C, SiC, Al_2O_3, SiO_2, MgO, TiB_2, and TiC are preferred in the production of aluminum matrix composites. Due to their economical production, silicon carbide (SiC-p) reinforced aluminum-based MCC's are among the most common and commercially available MCC's **[5]**. In addition to these reinforcements, carbon materials such as graphite, carbon fibers, carbon nanotubes (CNT's) and graphene (GNP) are prominent. Graphene has high fracture strength, good ductility and low thermal expansion coefficient, making it an ideal reinforcement for composite materials **[6]**. Many different methods produce MCC's. However, composite production using the powder metallurgy (PM) technique has recently been one of the most developed production methods **[7, 8]**. Powder metallurgy is a method of producing net shapes with many advantages such as low energy consumption, low material consumption, high precision and good stability. Complex parts that cannot be easily produced by traditional casting or machining methods can be processed with powder metallurgy **[9]**.

Powder metal-based compacts can be sintered using controlled atmosphere furnaces and ultra-high frequency induction systems (UHFIS) **[10]**. The heating process in induction systems (Fig. 1) is performed by applying an alternating current to an induction coil, which produces an alternating electromagnetic field around the coil. This field induces eddy currents within the metal object, leading to internal heat generation as a result of the material's electrical resistance **[26]**.

Induction systems are classified according to frequency intervals. According to the literature, the systems running 1-3 KHz and lower below are low-frequency, 3-50 kHz systems operating between moderate frequency, and 50-200 kHz systems are called high frequency systems **[27]**.

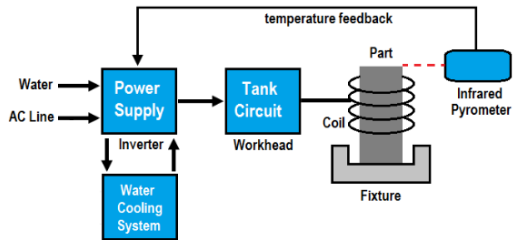

Figure 1. UHFIS **[28]**.

In addition, PM-based compacts can also be sintered by microwave sintering **[11, 12]**, plasma sintering, spark plasma sintering **[13]**, laser sintering and conventional sintering **[14, 15]**. Composites sintered by UHFIS are gaining prominence in terms of mechanical properties, processing time, energy costs and applicability.

This study investigated the effect of sintering aluminum matrix graphene (0.1% and 0.5%) and SiC (10% and 20%) reinforced hybrid composite with an ultra-high frequency induction heating system on mechanical and physical properties.

2. Materials and Methods

In the study, powders of the sizes and purities given in Table 2 were used for the Al-Cu powder mixture mixed at the macro level close to the AA2000 series chemical content.

Table 2. Powder properties.

Material	Purity	~ Particle size (µm)
Aluminum (Al)	99.9 %	+45 µm -63 µm
Copper (Cu)	99.9 %	<45 µm
Zinc (Zn)	99.3 %	>45 µm
Magnesium (Mg)	99.9 %	>45 µm
Silicon Carbide (SiC)	99.9 %	>45 µm
Graphene (GNP)	99.9 %	3nm -1.5 µm

The mixing ratios of aluminum-based hybrid composites are given in Table 3.

Table 3. Material content.

Material Code	2.1.10	2.5.20
Al %	84.4512	74.6794
Cu%	3.9547	3.4971
Mg%	1.3482	1.1922
Zn%	0.1258	0.1112
SiC%	10	20
Gr%	0.1	0.5

The powders used to produce composite specimens were mixed using the three-dimensional mixing system (3DMS) shown in Figure 2. To prevent agglomeration, 2 mm diameter Al_2O_3 balls were employed during the process. The mixing was carried out at a rotation speed of 250 rpm for a duration of 2 hours, with a ball to powder weight ratio of 1:1.

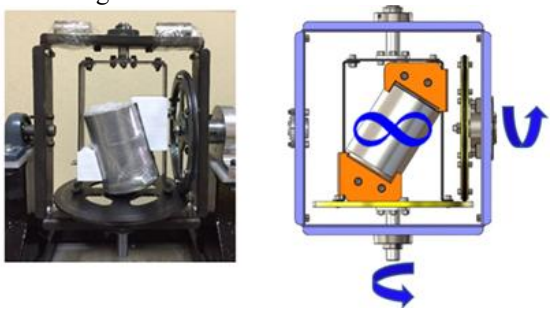

Figure 2. 3DMS **[16]**.

2.1. Preparation of composite and sintering

With the parameters in Table 5, Ø10x5mm sized samples were compacted by cold pressing and sintered in UHFIS, temperature and time determined according to the experimental sequence. The induction system

(Ceia Power Controller V3 and Power Cube 32/900) has a frequency level of 900 kHz, and 2.8 kW power. The heating temperature is carried out and stabilized with the infrared thermometer connected to the system.
TGA/DTA analyses were conducted using a Hitachi Exstar SII TG/DTA 7300 model thermogravimetric analyzer in the temperature range of 23–800 °C with a heating rate of 10 °C/min.
The experimental densities of the composites produced by powder metallurgy with Al-Cu matrix reinforced with 0.1 wt% graphene and 10 wt% SiC, Al-Cu matrix reinforced with 0.5 wt% graphene and 20 wt% SiC and sintered by UHFIS method were made according to Archimedes principle in accordance with ASTM B962-17 standard (Eq. 1).

$$\rho_D = \left(\frac{m_D}{m_L - m_W}\right)\rho_{water} \quad (1)$$

(m_D=Dry mass of composites, m_L=Mass saturated with water in the liquid, m_W= Measured suspended mass in water)

Macro hardness tests were carried out in accordance with ASTM E10 standards in the EMCO-TEST DuraVision G5 hardness tester using a 2 mm diameter ball under a 62.5 kg load. The hardened samples were subjected to a metallography process. Then, microstructure images were taken with the help of Nikon brand Eclipse LV150 model optical microscope.

2.2 Experimental design and experiments

The Taguchi method also reduces the number of experiments **[20]**. The production parameters and levels used in the experiments and selected as factors are given in Table 4. Sintering temperatures were selected according to TGA/DTA analysis. Compression pressures used for aluminum-based composites in the literature vary between 300-600 MPa. Compression pressure in the studies, Judge et al. **[29]** 300 MPa, Çavdar and Akkurt **[11]** 400 MPa, Şenel et al. **[13]**, Levent et al. **[23]** 600 MPa. In the studies, the pressure amount to be formed by 10mm diameter staple on the sample was selected as 80 (326 MPa), 90 (367 MPa) and 100 (408 MPa). The parameters commonly used in literature have been selected for sintering times.

Table 4. Parameters and levels used in the experiments.

Symbol	Parameters	Levels		
		1	2	3
A	Pressure (bar)	80	90	100
B	Sintering temperature (°C)	580	600	620
C	Sintering time (min)	5	7	10

L9 (3^3) orthogonal array was selected for the experimental design. For complete factorial experimental design, 9 experiments were carried out using Taguchi L9 orthogonal array instead of 27.
The experimental design created according to the factors and levels for the parameters used to find the compression pressure, sintering temperature and sintering time of the hybrid composite materials coded 2.1.10 and 2.5.20 planned to be produced is shown in Table 5.

Table 5. Experimental design.

	Factors		
Experiment Number	A Compression Pressure (bar)	B Sintering Temperature (°C)	C Sintering Time (min)
N1	80	580	5
N2	80	600	7
N3	80	620	10
N4	90	580	7
N5	90	600	10
N6	90	620	5
N7	100	580	10
N8	100	600	5
N9	100	620	7

3. Results

3.1. TGA/DTA analyses of powders

Thermogravimetric Analysis and Differential Thermal Analysis (TGA/DTA) are employed to determine mass losses or gains, as well as melting temperatures, as a function of temperature or time. In the study by PS Liu et al., it is seen that the sintering temperature is 0.6-0.8 times above the melting temperature of the primary matrix material when strength, hardness, toughness, ductility, porosity and especially mechanical strength are taken into consideration **[17]**. At the same time, German states that the sintering temperature should be below the melting temperature of the matrix element. From this point of view, since it would not be correct to determine an apparent sintering temperature for the hybrid composites produced, it was found appropriate to perform TGA/DTA analysis of the mixed powders to determine the melting temperature of the hybrid composite powders **[18]**.
Before producing Al-Cu matrix graphene and SiC-reinforced composites, TGA/DTA analyses were performed to determine the melting temperatures of powder mixtures with codes 2.1.10 and 2.5.20. The results of TGA/DTA analyses for the mass gains and losses of Al-Cu matrix graphene and SiC-reinforced composite powders as a function of temperature and time are given below (Figures 3a and 3b).

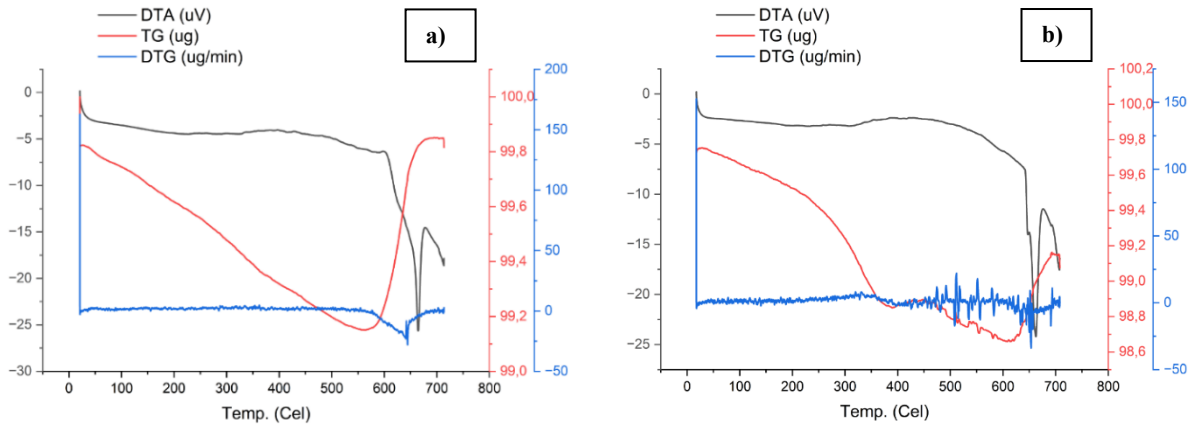

Figure 3. TGA/DTA analysis results of mixture powder a) 2.1.10, b) 2.5.20.

When the TGA/DTA analysis results of the mixture powder coded 2.1.10 shown in Figure 3a is examined, it is seen that mass losses occur between 23 and 560 ◦C temperatures. At 560 ◦C, 0.85% mass loss was determined. Mass increases start above this temperature level. DTA curve is analyzed, an endothermic peak is observed at 225 ◦C, resulting from the removal of organics and corresponding to the melting of the mixed powder at 664 ◦C.

When the TGA/DTA result of the mixture powder coded 2.5.20, shown in Figure 3b, is analyzed, mass losses occur between 23 and 605 ◦C. Mass losses were determined as 1.15% at 390 ◦C and 1.35% at 605 ◦C. When the DTA curve is analyzed, it shows an endothermic peak at 662 ◦C, corresponding to the melting of the mixed powder. When the TGA/DTA analyses are evaluated in general, increased mass losses are observed with increasing graphene reinforcement. Smaller carbon particles have a higher number of edge regions per mass unit. This means smaller carbon particles are more reactive and sensitive to the combustion process than larger particles **[19]**. Since the mass increases in the melting point region in the mixed powders are observed to start at approximately 600 ◦C, this temperature was selected as an intermediate value for sintering experiments and sintered at 580, 600 and 620 ◦C.

3.2. Density results

The relative density values of 2.1.10 and 2.5.20 composites, whose densities were measured by the Archimedes principle, are given in Table 6. The highest relative density value, 99.08%, was obtained in 0.1% graphene and 10% SiC reinforced composites in graphene and SiC reinforced samples. The lowest relative density value was 92.45% in 0.5% graphene and 20% SiC-reinforced composites.

Table 6. Relative density values of composite materials.

Exp. No	2.1.10	2.5.20
1	%97,78	%98,18
2	%96,62	%96,37
3	%93,54	%93,43
4	%95,75	%95,37
5	%96,87	%96,94
6	%94,36	%95,57
7	%96,18	%94,11
8	%99,08	%96,79
9	%96,51	%92,45

3.3. Hardness results

The averages hardness obtained from the surfaces and different regions of 0.1% graphene-10% SiC and 0.5% graphene-20% SiC reinforced composites with Al-Cu matrix are given in Table 7.

Table 7. Average hardness values of hybrid composites.

Experiment No	Hardness Results (HB)	
	2.1.10	2.5.20
N1	85.7	78,6
N2	84.3	80,5
N3	76.9	68,6
N4	78.7	78,7
N5	70.8	88,5
N6	69.4	84,6
N7	90.4	70,4
N8	87.4	103,5
N9	82.3	56,4

According to Figure 4a, the highest hardness value in the 2.1.10 composite was 90.4 HB in the sample coded N7 sintered at 100 bar compression pressure and 580°C for 10 min. In the study by Çavdar et al., graphene was added to aluminum nanoparticles in the 40-50 nm size range at the rate of 0.1-0.2-0.3-0.4-0.5-0.6-0.6-0.8-1

and 2 wt% **[11]**. Under 400 MPa pressure, it was compressed by the cold isostatic pressing method. Then, it sintered at 620°C under argon gas for 1 hour. The highest hardness value was 68 HV with 0.8% graphene addition. Leszczynska et al., measured the hardness of Al-5%SiC composite as 30.5 HV and Al-10SiC composite as 31.7 HV, while pure Al sintered conventionally at 620°C for 1 hour had a hardness of 27.7 HV **[22]**. Finally, Gezici et al., produced B4C and SiC hybrid reinforced Al-Cu-Mg-Si alloy matrix composites using the microwave sintering method at 550°C sintering temperature for 60 minutes. In the hybrid composites produced, 3, 6, 9, and 12 wt% SiC were used while keeping the B_4C ratio constant. The highest hardness value of 117.2 HV was obtained in 12 wt% SiC reinforced hybrid material **[23]**.

According to Figure 4b, the highest hardness value in the 2.5.20 composite was 103.5 HB in the sample coded N8 sintered at 100 bar compression pressure and 600°C for 5 min. Hsieh et al. sintered the composite obtained by adding 25 wt% reinforcement to Al 6061 at 525°C for 3 min by the UHFIS method. With 0.25 % graphene reinforcement, hardness increased from 60.1 HV to 68 HV **[24]**.

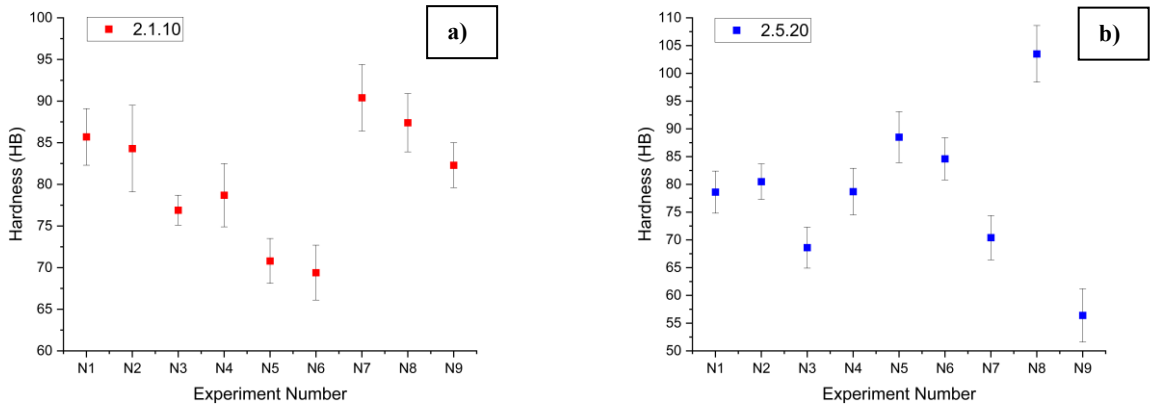

Figure 4. Hardness values of hybrid composites a) 2.1.10, b) 2.5.20.

3.4. Evaluation of Experimental Results by Analysis of Variance

The effect of compression pressure, sintering temperature and sintering time on the hardness of the material was analyzed and evaluated by ANOVA method. The ANOVA values for the hardness values obtained as a result of varying compression pressure, sintering temperature and sintering time of the composites are given in Table 6.

When the hardness values of the 2.1.10 composite given in Table 6 are compared according to the importance of the parameters for the ANOVA results, the sintering temperature in the table is effective. When the effects of the parameters were analyzed, compression pressure was 7,21%, sintering temperature 27,40%, sintering time 0,78%, and error 1,38%.

When the hardness values of the 2.5.20 composite are compared according to the importance of the parameters for ANOVA results, the sintering time in the table is effective. When evaluated in terms of the effects of the parameters, compression pressure was 0,08%, sintering temperature 3,85%, sintering time 14,22% and error 8,81%.

The best compression pressure reached due to Taguchi experiments was determined as 100 bar. The best sintering parameters for 2.1.10 composite were determined as 10 min at 580°C and 5 min at 600°C for 2.5.20 composite.

3.5. Regression Method for Experimental Results

In this study, the level of relationship between hardness and control factors was determined using a polynomial regression model. Multiple regression analysis obtains the prediction equations of continuous dependent variables obtained through experimental designs with each combination of control factors **[21].**

Celal Bayar University Journal of Science
Volume 21, Issue 4, 2025, p 118-127
Doi: 10.18466/cbayarfbe.1666717

Table 8. ANOVA results of hardness values obtained in the experiments.

Factors	Degrees of Freedom (DF)	Sum of Squares (SS)	Mean of Squares (MS)	F-Value	P-Value	Factor Effect (%)
2.1.10						
Compression pressure	1	31,282	263,760	88,18	0,011	7,21
Sintering temperature	1	118,815	0,024	0,01	0,937	27,40
Sintering time	1	3,380	3,491	1,17	0,393	0,78
Error	2	5,982	2,991	-	-	1,38
Total	8	433,589	-	-	-	-
2.5.20						
Compression pressure	1	1,13	116,13	1,86	0,306	0,08
Sintering temperature	1	54,60	640,74	10,27	0,085	3,85
Sintering time	1	201,48	316,67	5,07	0,153	14,22
Error	2	124,82	62,41	-	-	8,81
Total	8	1417,08	-	-	-	-

2.1.10 The mathematical equation derived for the second-order regression model for predicting the hardness of the composite is given in Eq. 2. R^2 value for the equation of hardness value of 2.1.10 composite was obtained as 98,62%.

2.5.20 The mathematical equation derived for the second-order regression model in order to predict the hardness of the composite is given in Eq. 3. 2.5.20 R^2 value for the hardness value equation of the composite was obtained as 91,19%.

$$H_{(2.1.10)} = 951 - (20{,}68P) + (0{,}33T) + (3{,}37ST) + (0{,}1162P^2) - (0.00046T^2) - (0.242ST^2) \quad (2)$$

$$H_{(2.5.20)} = -16467 + (13{,}7P) + (53{,}7T) - (32{,}1ST) - (0{,}076P^2) - (0{,}0449T^2) + (1{,}968ST^2) \quad (3)$$

(H: Hardness, P: Pressure, T: Temperature, ST: Sintering Time)

3.6. Microstructure analysis

The hardness results of the 2.1.10 composites in Figure 4 show that the lowest hardness value is in the N6 sample. When the microstructure images of the N6 sample in Figures 5a and 5a[1] are examined, it is revealed that agglomeration occur in the samples, negatively affecting the hardness results. The highest value belonging to the same group of powder mixture was in the N7 sample in Figure 5d. In Figures 5b, 5c and 5e, it is seen that SiC particles are homogeneously distributed, but there are agglomerates in the graphene additive. Despite this situation, the best properties occurred here. In addition, according to the hardness results, N1, N2, and N8 samples give results close to N7. When Figures 5b, 5c and 5e are examined, it is seen that they show similar properties to N7.

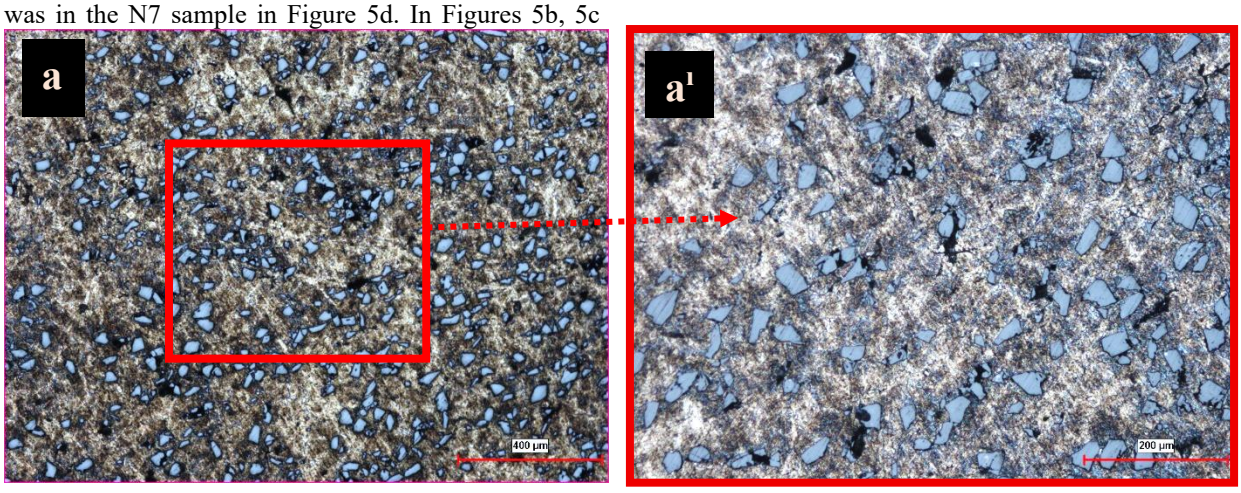

Celal Bayar University Journal of Science
Volume 21, Issue 4, 2025, p 118-127
Doi: 10.18466/cbayarfbe.1666717

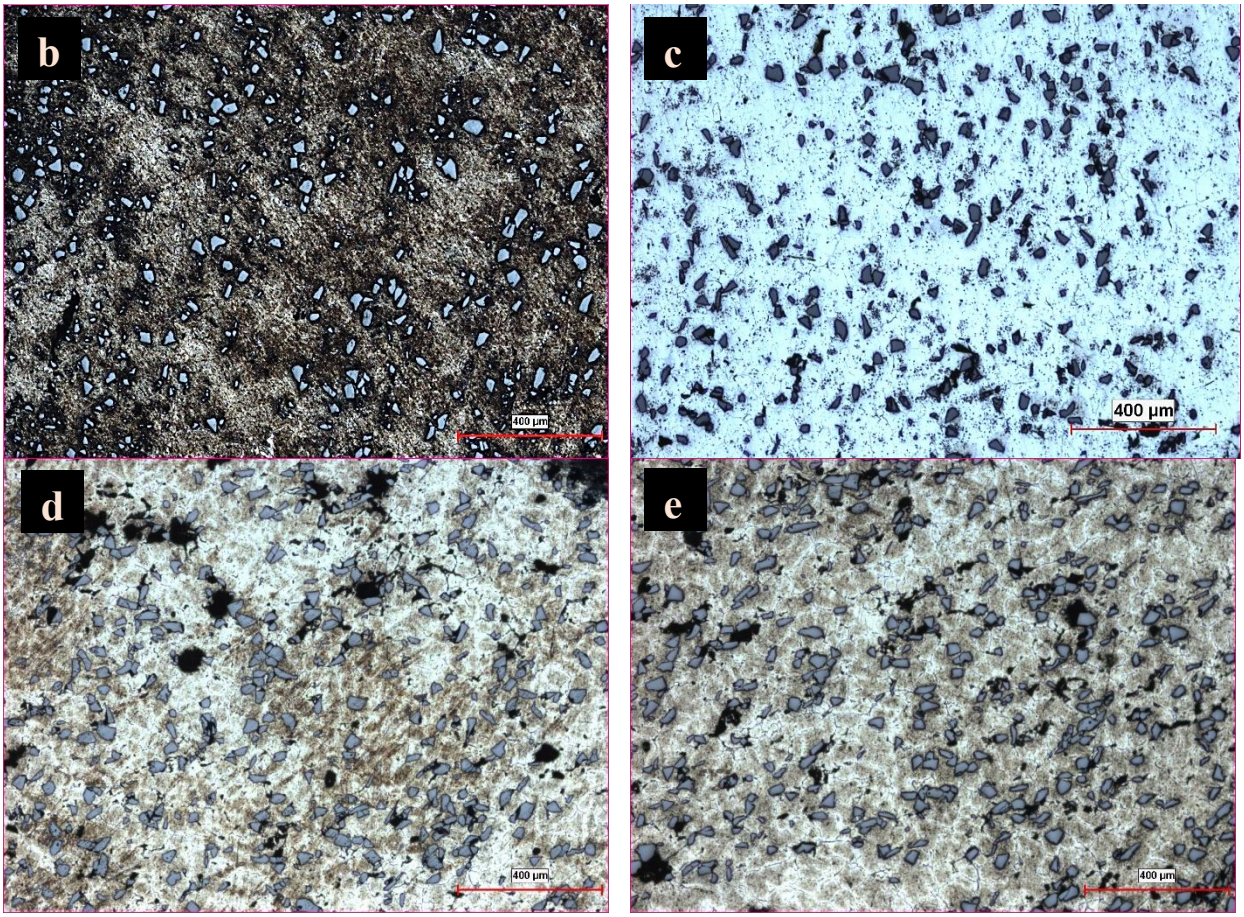

Figure 5. 2.1.10 composite microstructure images a, a[1]) N6, b) N1, c) N2, d) N7, e) N8

When the hardness results of the 2.5.20 composites in Figure 4 are examined, it is seen that the lowest hardness value is in the samples coded N3 and N9. Figures 6a and 6a[1] show the microstructure of sample N3, and Figures 6b shows the microstructure of sample N9. It is understood that cracks and agglomeration occur in the microstructure of both groups. The regions where the cracks are located are marked with arrows in a[1] and b[1]. The highest value belonging to the same group of powder mixture occurred in the sample coded N8. Figure 6d show that SiC particles are homogeneously distributed. It is also seen that it has a high-density structure. It is observed that graphene shows agglomeration in places but settles at the grain boundaries. This result led to the best hardness value. The graphene distribution of sample N5, which has the second highest hardness value, showed more agglomeration tendency, unlike sample N8 (Figure 6c).

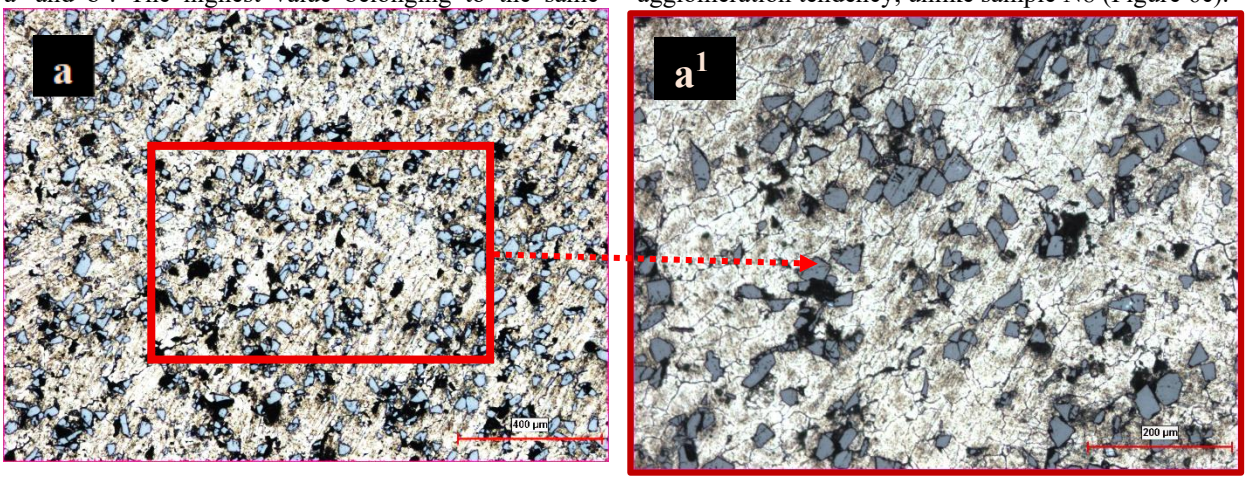

Celal Bayar University Journal of Science
Volume 21, Issue 4, 2025, p 118-127
Doi: 10.18466/cbayarfbe.1666717

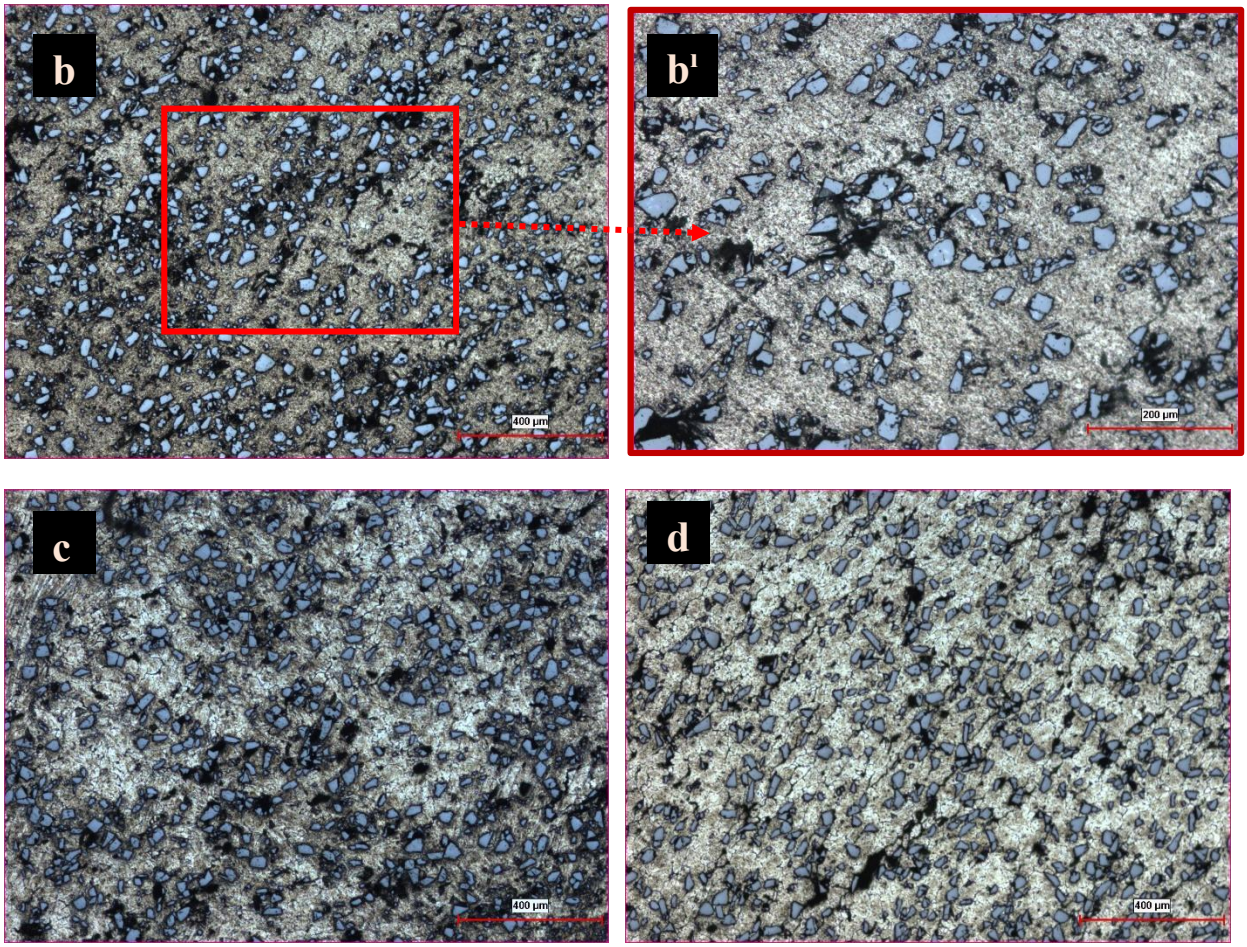

Figure 6. Microstructure images of 2.5.20 composite a-a[1]) N3, b-b[1]) N9, c) N5; d) N8.

4. Discussion

In this study, the mechanical properties of aluminum matrix hybrid composites reinforced with graphene and SiC, sintered using an ultra-high frequency induction heating system (UHFIS), were investigated. The findings were evaluated by comparing them with similar studies in literature.

Firstly, the effects of production parameters such as pressure, sintering temperature, and sintering time on composite hardness were examined using ANOVA analysis. The results showed that sintering temperature was the most significant factor, with an impact of 27,40% on the 2.1.10 composite and sintering time was the most significant factor with 14,22% on the 2.5.20 composite.

The effect of sintering temperature was evaluated, revealing that 580°C was the optimal value for 2.1.10 composite and 600 °C for 2.5.20 composite. This result is consistent with the study by Leszczynska et al., which reported that the 600-620 °C temperature range provided optimal mechanical properties for SiC-reinforced aluminum composites **[25]**.

The use of different ratios of graphene and SiC caused notable variations in mechanical properties. The composite containing 0.5% graphene and 20% SiC exhibited higher hardness, supporting the hardness-enhancing effect of graphene highlighted by Hsieh et al. **[26]**. Moreover, microstructure analyses indicated that the homogeneous distribution of graphene plays a crucial role in improving mechanical properties.

The high relative density achieved through the powder metallurgy (PM) method plays a significant role in enhancing the mechanical properties of composite materials **[30]**. When the results obtained from the experiments of the composites of 2.1.10 and 2.5.20 were examined, a positive relationship was observed between the hardness values and the relative density. It is seen that hardness values increase in increasing relative densities. The hardness of aluminum matrix composite materials is controlled by dislocation mechanisms. Nano is the size of the graphene, which has a size and a plate structure, causes an increase in the dislocation intensity of the composite. Hardness is directly associated with the dislocation intensity and raises hardness values **[30]**.

The hardness and density values of the composite coded 2.5.20 in sample N9 (56.4 HB – 92.45%) were observed to be lower compared to the other samples. As the graphene content increases, the agglomeration of graphene leads to a decrease in hardness values **[30]**. The addition of graphene can cause agglomeration within the internal structure, resulting in increased

porosity, weakened mechanical properties, and crack formation **[31].** Since the increase in hardness values is directly related to the low porosity of metal matrix composites, the decrease in hardness with increasing graphene content confirms this relationship **[32]**. This phenomenon arises because excessive graphene agglomerates are a primary source of damage such as cracks in composites **[33]**.
Microstructure images demonstrated that high pressure and appropriate sintering times reduced crack formation, thereby improving mechanical properties. This finding aligns with similar results reported in hybrid composite studies by Gezici et al. **[23]**.
These evaluations largely confirm the tested hypotheses. Proper selection of the combination of pressure, temperature, and sintering time can significantly enhance the mechanical properties of hybrid composites produced using the UHFIS method. These results increase the feasibility of using aluminum matrix composites reinforced with graphene and SiC in advanced engineering applications.

5. Conclusion

According to the experimental results of Al-Cu-based hybrid composites with minimum and maximum reinforcement ratios sintered by the UHFIS method, it is seen that much more successful results have been achieved compared to the literature. The following results were obtained from sintering graphene and SiC-reinforced aluminum matrix hybrid composites with UHFIS.

- According to the ANOVA analysis, it is understood that the most influential parameters in the production of composites are sintering temperature and time.
- The best compression pressure reached due to Taguchi experiments was determined to be 100 bar.
- According to Taguchi's results, the best sintering parameters for 2.1.10 composite were determined as 10 min at 580°C and 5 min at 600°C for 2.5.20 composite.
- The highest hardness value of 2.1.10 composite was determined as 90.4 HB in sample N7 sintered at 100 bar compression pressure and 580°C for 10 min.
- In the 2.5.20 composite, the highest hardness value was determined as 103.5 HB in the sample coded N8 sintered at 100 bar compression pressure and 600°C for 5 min.

Acknowledgement

This study is supported by "TUBITAK 1002-A Short term Support Module Project No: 224M442"

Author's Contributions

Büşranur KESER: Performed the experiments and results analysis, manuscript preparation.

Gürkan SOY: Prepared experimental method, performed the experiments and results analysis and interpretation of results.

Selda AKGÜN KAYRAL: Supervised the experiment's progress, interpretation of results and helped in manuscript preparation.

Ethics

There are no ethical issues after the publication of this manuscript.

References

[1] Uygur, İ. Environmentally assisted fatigue response of Al-Cu-Mg-Mn with SiC particulate metal matrix composites; University of Wales Swansea,1999.

[2] Chen Y. S., Chen T. J., Zhang S. Q., & Li P. B. (2015). Effect of ball milling on microstructural evolution during partial remelting of 6061 aluminum alloy prepared by cold pressing of alloy powders, *Trans. Nonferrous Met. Soc. China (English Ed.*, vol. 25, no. 7, pp. 2113–2121.(https://doi.org/10.1016/S1003-6326(15)63822-5)

[3] Kretschmer J. (1988). "Composites in automotive applications state of the art and prospects" *Mater. Sci. Technol. (United Kingdom)*, vol. 4, no. 9, pp. 757–767. (https://doi.org/10.1179/mst.1988.4.9.757)

[4] Şenel M.C., Gürbüz M. & Koç E. (2018). "The Investigation on Mechanical Properties of Al-Si_3N_4 Metal Matrix Composites Fabricated by Powder Metallurgy Method," *Eng. Mach.*, vol. 59, no. 693, pp. 33–46.

[5] Bedir F. & Ogel B. "Investigation of hardness, microstructure and wear properties of SiC-p reinforced Al composites" *11th International Conference on Machine Design and Production,*2004.

[6] Du X. Zheng K. & Liu F. (2018). "Microstructure and mechanical properties of graphene-reinforced aluminum-matrix composites" *Mater.Tehnol.*, vol.52, no. 6, pp.763–768. (https://doi.org/10.17222/mit.2018.021)

[7] Orhan A. Gür A. K. & Çaligülü U. (2007). "Produced by hot pressing method of composites made with Al matrix B_4C reinforcement" *Electron. J. Mach. Technol.*, vol. 2007, no. 4, pp. 8–13.

[8] Kumar N. Bharti A. & Saxena K. K. (2021). "A Re-Investigation: Effect of powder metallurgy parameters on the physical and mechanical properties of aluminium matrix composites" in *Materials Today: Proceedings*, vol. 44, pp. 2188–2193. (https://doi.org/10.1016/j.matpr.2020.12.351)

[9] ren Ke B. *et al.* (2021). "Powder metallurgy of high-entropy alloys and related composites: A short review" *Int. J. Miner. Metall. Mater.*, vol. 28, no. 6, pp. 931–943. (https://doi.org/10.1007/s12613-020-2221-y)

[10] Madhan M. & Prabhakaran G. (2019). "Microwave versus conventional sintering: Microstructure and mechanical properties of Al_2O_3 -SiC ceramic composites" *Bol. la Soc. Esp. Ceram. y Vidr.*, vol. 58, no. 1, pp. 14–22. (https://doi.org/10.1016/j.bsecv.2018.06.001)

[11] Çavdar U. & Akkurt O. (2018). "The Effect of Sintering on the Microstructure, Hardness, and Tribological Behavior of Aluminum–Graphene Nanoplatelet Powder Composites," *Powder Metall. Met. Ceram.*, vol. 57, no. 5–6, pp. 265–271. (https://doi.org/10.1007/s11106-018-9978-9)

[12] Kare D. Chintada S. Dora S. P. & Swain P. K. (2021). "Damping characteristics of pure aluminum: A comparison of microwave and conventional sintering" *Met. Powder Rep.*, vol. 76, no. 6, pp. 22–25. (https://doi.org/10.1016/S0026-0657(21)00299-X)

[13] Şenel M. C. Gürbüz M. & Koç E. (2017). "The fabrication and characterization of graphene reinforced aluminum composites" *Pamukkale Univ. J. Eng. Sci.*, vol. 23, no. 8, pp. 974–978. (https://doi.org/10.5505/pajes.2017.65902)

[14] Rashad M. Pan F. Yu Z. Asif M. Lin H. & Pan R. (2015). "Investigation on microstructural, mechanical and electrochemical properties of aluminum composites reinforced with graphene nanoplatelets" *Prog. Nat. Sci. Mater. Int.*, vol. 25, no. 5, pp. 460–470. (https://doi.org/10.1016/j.pnsc.2015.09.005)

[15] Nieto A. Huang L. Han Y. H. & Schoenung J. M. (2015). "Sintering behavior of spark plasma sintered alumina with graphene nanoplatelet reinforcement" *Ceram. Int.*, vol. 41, no. 4, pp. 5926–5936. (https://doi.org/10.1016/j.ceramint.2015.01.027)

[16] Soy G. & Korucu S. (2022). "Investigations on the Mechanical Alloying Properties of Al 2024 Alloy by Three-Dimensional Ball Mill" *Surf. Rev. Lett.*, vol. 29, no. 11. (https://doi.org/10.1142/S0218625X22501426)

[17] Liu P. S. & Chen G. F. (2014). "Making Porous Metals," in *Porous Materials*, Butterworth-Heinemann, pp. 21–112. (https://doi.org/10.1016/B978-0-12-407788-1.00002-2)

[18] German R. M. (2007). "Powder Metallurgy and Particulate Material Transactions," in *Powder Metallurgy & Particulate Materials Processing*, S. Sarıtaş, M. Türker, and N. Durlu, Eds. Ankara: Turkish Powder Metallurgy Association Publications.

[19] Lal S. Kumar S. Kumar A. Patel L & Aniruddha. (2022). "Fabrication and characterization of hybrid metal matrix composite Al-2014/SiC/fly ash fabricated using stir casting process" *Mater. Today, Proc.*, vol. 49, pp. 3155–3163. (https://doi.org/10.1016/j.matpr.2020.11.168)

[20] Samtaş G. & Korucu S. (2022). "Optimization of cutting parameters for surface roughness in milling of cryogenic treated EN AW 5754 ($AlMg_3$) aluminum alloy" *J. Polytech.*, vol. 22, no. 3, pp. 665–673. (https://doi.org/10.2339/politeknik.457957)

[21] Samtaş G. & Korucu S. (2019). "The Optimization of Cutting Parameters Using Taguchi Method in Milling of Tempered Aluminum 5754 Alloy" *Düzce Univ. J. Sci. Technol.*, vol. 7, pp. 45–60. (https://doi.org/ 10.24425/bpasts.2019.130179)

[22] Leszczyńska-Madej B. Garbiec D. & Madej M. (2019). "Effect of sintering temperature on microstructure and selected properties of spark plasma sintered Al-SiC composites" *Vacuum*, vol. 164, pp. 250–255. (https://doi.org/10.1016/j.vacuum.2019.03.033)

[23] Gezici L. U. Özer E. Sarpkaya I. & Çavdar U. (2022). "The effect of SiC content on microstructural and tribological properties of sintered B_4C and SiC reinforced Al-Cu-Mg-Si matrix hybrid composites" *Mater. Test.*, vol. 64, no. 4, pp. 502–512. (https://doi.org/10.1016/j.vacuum.2019.03.033)

[24] Çavdar U. Atik E. (2011). "Geleneksel ve hızlı sinterleme yöntemleri", CBÜ Soma Meslek Yüksekokulu Teknik Bilimler Dergisi, Cilt 1, Sayı 15, Sayfa 1-10.

[25] Leszczyńska-Madej B. Tylek A. & Wąsik M. (2015). "Mikrostruktura i właściwości kompozytów na osnowie stopu aluminium umacnianych węglikiem krzemu" Rudy i Metale Nieżelazne Recykling, Cilt 60. (https://doi.org/10.15199/67.2015.5.3)

[26] Hsieh C. T. Ho Y. C. Wang H. Sugiyama S. & Yanagimoto J. (2020). "Mechanical and tribological characterization of nanostructured graphene sheets/A6061 composites fabricated by induction sintering and hot extrusion" *Mater. Sci. Eng. A*, vol. 786, p. 138998. (https://doi.org/10.1016/j.msea.2020.138998)

[27] Taştan M. Gökozan H. Sarı Çavdar P. Soy G. & Çavdar U. (2019). "Analysis of artificial aging with induction and energy costs of 6082 Al and 7075 Al materials" *Revista De Metalurgia*, *55*(1), e137. (https://doi.org/10.3989/revmetalm.137)

[28] Taştan M. Gökozan H. Sarı Çavdar P. Soy G. & Çavdar U. (2020). "Cost analysis of T6 induction heat treatment for the aluminum-copper powder metal compacts" *Science of Sintering*, vol.52, no.1, pp.77-85. (https://doi.org/10.2298/sos2001077t)

[29] Judge W. D. Bishop D. P. & Kipouros G. J. (2017). "Industrial sintering response and microstructural characterization of aluminum powder metallurgy alloy Alumix 123". *Metallography, Microstructure, and Analysis*, vol. 6, pp. 375-382. (https://doi.org/10.1007/s13632-017-0379-0)

[30] Şenel M. C. Gürbüz M. & Koc E. (2018). "Fabrication and characterization of synergistic Al-SiC-GNPs hybrid composites." *Composites Part B: Engineering* 154, 1-9. (https://doi.org/10.1016/j.compositesb.2018.07.035)

[31] Anthony Xavior M. Ranganathan N. Kumar P. Joel H.G. Ashwath.P. (2018). "Mechanical properties evaluation of hot extruded AA 2024–Graphene Nanocomposites." *Materials Today: Proceedings* 5.5, 12519-12524. (https://doi.org/10.1016/j.matpr.2018.02.233)

[32] Swamy A. R. K. Ramesha A. Kumar G. V. & Prakash J. N. (2011)."Effect of particulate reinforcements on the mechanical properties of Al6061-WC and Al6061-Gr MMCs." *Journal of minerals and materials characterization and engineering* 10.12, 1141-1152. (https://doi.org/10.4236/jmmce.2011.1012087)

[33] Huang Z. Yan H. & Xiong J. (2022). "Analysis of microstructure and mechanical properties of graphene nanoplatelet reinforced 2024Al alloy." *Materials Science and Engineering: A* 832, 142466. (https://doi.org/10.1016/j.msea.2021.142466)